Available online at www.sciencedirect.com

SCIENCE DIRECT®

ELSEVIER

International Journal of Solids and Structures 42 (2005) 4555–4573

INTERNATIONAL JOURNAL OF SOLIDS and STRUCTURES

www.elsevier.com/locate/ijsolstr

On a moving interface crack with a contact zone in a piezoelectric bimaterial

K.P. Herrmann [a], A.V. Komarov [b], V.V. Loboda [b,*]

[a] *Lehrstuhl fuer Technische Mechanik, Paderborn University, Pohlweg 47-49, D-33098 Paderborn, Germany*
[b] *Department of Theoretical and Applied Mechanics, National University, Nauchni Str. 13, Dniepropetrovsk 49050, Ukraine*

Received 26 October 2004; received in revised form 4 February 2005
Available online 19 March 2005

Abstract

An inplane problem for a crack moving with constant subsonic speed along the interface of two piezoelectric materials is considered. A mechanically frictionless and electrically permeable contact zone is assumed at the right crack tip whilst for the open part of the crack both electrically permeable and electrically insulated conditions are considered. In the first case a moving concentrated loading is prescribed at the crack faces and in the second case an additional electrical charge at the crack faces is prescribed as well. The main attention is devoted to electrically permeable crack faces. Introducing a moving coordinate system at the leading crack tip the corresponding inhomogeneous combined Dirichlet–Riemann problem is formulated and solved exactly for this case. All electromechanical characteristics at the interface are presented in a closed form for arbitrary contact zone lengths, and further, the transcendental equation for the determination of the real contact zone length is derived. As a particular case of the obtained solution a semi-infinite crack with a contact zone is considered. The numerical analysis performed for a certain piezoelectric bimaterial showed an essential increase of the contact zone length and the associated stress intensity factor especially for the near-critical speed region. Similar investigations have been performed for an electrically insulated crack and the same behavior of the above mentioned parameters is observed.

Keywords: Moving interface crack; Contact zone; Piezoelectric material

* Corresponding author. Tel.: +38 562 469291; fax: +38 56 7765833.
E-mail addresses: jherr1@ltm.upb.de (K.P. Herrmann), loboda@mail.dsu.dp.ua (V.V. Loboda).

0020-7683/$ - see front matter
doi:10.1016/j.ijsolstr.2005.02.003

1. Introduction

Piezoelectric materials due to their intrinsic thermo-electro-mechanical coupling are referred to the most actively developed contemporary materials which are widely used in engineering as sensors, transducers and actuators. However, an adhesion of isotropic, anisotropic or piezoelectric components leads usually to the appearance of interface cracks which can situate in the interfaces till the appearance of certain critical conditions which lead to growth and propagation of a crack into the matrix or more really along the interfaces. The explanation of the static interface cracks behavior and their dynamic propagation along the interfaces of multiphase materials under mechanical, thermal and electrical loadings forms an important basis for an assessment of the strength of real constructions.

The first solution of a dynamic steady state crack problem was given by Yoffe (1951) who considered a crack of a finite length moving with constant velocity in an infinite isotropic solid. The investigation of an interface crack propagation along the interface of two isotropic solids has been initiated by Gol'dstein (1966) and was continued by Willis (1971), Atkinson (1977) and other authors. In these papers various loadings and different crack velocities with respect to the Rayleigh wave speed have been considered. The Lekhnitskii (1963), Eshelby et al. (1953) and Stroh (1958) formalisms have been applied by Wu (1991) and Yang et al. (1991) for the investigation of an extending interface crack in an anisotropic bimaterial along a straight interface. The generalization of Yoffe's (1951) and Gol'dstein's (1966) problems upon the investigation of an interface crack propagating along an interface of two anisotropic materials has been particularly performed by Yang et al. (1991).

An effect of the temperature upon an interface crack running along the interface of isotropic and anisotropic materials has been studied in the papers by Herrmann and Noe (1992, 1993, 1995) and Noe and Herrmann (1993, 1997). Experimental investigations and theoretical studies of thermoelastic problems for a crack propagating along a curvilinear interface has been performed in these papers by means of the method of caustics and the analytical approach based upon the Lekhnitskii–Eshelby–Stroh formalism.

It is worth to note that to our knowledge the results concerning the propagation of an interface crack along the interface between two piezoelectric materials or between piezoelectric and nonpiezoelectric materials are practically absent in the literature. Only the papers by Chen et al. (1998) and Wang et al. (2003) where an anti-plane problem for a Griffith crack moving along an interface of a piezoelectric bimaterial was studied as well as by Shen et al. (2000) considering the power of the stress field singularities concerning an in-plane electrically permeable crack running between two piezoelectric materials can be referred to on this subject.

Moreover, all results mentioned above were obtained in the framework of a so-called "open crack" model for an interface crack (Williams, 1959) possessing for a subsonic in-plane case the oscillating singularity at the propagating crack tip. Such an approach is suitable if the interpenetration zone of the crack faces remains small with respect to the current crack length or some other characteristic dimensions of the problem. For a static case this condition is usually satisfied for real materials provided the absence of essential shear and thermal fields. However, for a propagating crack the bimaterial "constant" ε (parameter of oscillation) becomes dependent on the crack speed v and according to Yang et al. (1991) this parameter can rapidly grow if v tends to the Rayleigh wave speed of one bimaterial component.

The contact zone model for an elastostatic interface crack has been suggested by Comninou (1977) and was further developed in an analytical way by Simonov (1985), Gautesen and Dundurs (1988), Loboda (1993) and other authors. An exact analytical investigation of the contact zone model for an interface crack in an anisotropic bimaterial has been performed by Herrmann and Loboda (1999) and a similar investigation for a piezoelectric bimaterial has been done by Herrmann and Loboda (2000) and Herrmann et al. (2001) for electrically insulated and electrically permeable cracks, respectively. A moving semi-infinite interface crack in an isotropic bimaterial under a concentrated loading on its faces was analyzed by Simonov (1983) by taking into account the contact of the crack faces at the leading crack tip. The dynamic contact problem for an orthotropic half-plane and an orthotropic bimaterial plane with different types of boundary conditions at the material interface was investigated by Nakhmejn and Nuller (1990). Particularly the problem of the delaminating of a rigid stamp from a semi-infinite orthotropic plane with an account of the open, closed and bonded zones at its interface was analyzed in this work. An interface crack moving along an interface with an intersonic speed was considered by Huang et al. (1998). But it is worth to note that for an intersonic case the bimaterial parameter ε becomes a complex value and the mathematical peculiarities of the problem become completely different from the associated one in the subsonic case. Herrmann et al. (2004) presented an exact analytical solution for an interface crack between two anisotropic materials moving along an interface with a subsonic speed.

In the present investigation the problem of a moving interface crack in a piezoelectric bimaterial with an account of a contact of the crack faces at the leading crack tip is considered. The cases of a finite and a semi-infinite crack length are under consideration, and the crack speed is restricted to a subsonic regime.

2. Basic relations for a piezoelectric solid with an account of a moving coordinate system

According to Parton and Kudryavtsev (1988) the dynamic constitutive equations for a piezoelectric material in a fixed coordinate system (X_1, X_2, X_3) can be written in the form

$$(c_{ijrs}u_r + e_{sji}\varphi)_{,si} = \rho\frac{\partial^2 u_j}{\partial t^2}, \tag{1a}$$

$$(-\varepsilon_{is}\varphi + e_{irs}u_r)_{,si} = 0, \tag{1b}$$

$$\sigma_{ij} = C_{ijrs}u_{r,s} + e_{sji}\varphi_{,s}, \tag{2a}$$

$$D_i = -\varepsilon_{is}\varphi_{,s} + e_{irs}u_{r,s}, \tag{2b}$$

where u_k, φ, σ_{ij}, D_i, are the elastic displacements, electric potential, stresses and electric displacements, respectively, and ρ is the material density. Furthermore, c_{ijkl}, e_{lij} and ε_{ij} are the elastic modulo, piezoelectric constants and dielectric constants, respectively. Small subscripts in (1)–(2) and afterwards are always ranging from 1 to 3 and Einstein's summation convention on repeated Latin suffixes has been used. Further, the right hand side of Eq. (1b) equals zero because the magnetic effects can be neglected for a study of elastic waves and the so-called quasi-static approximation for the electrical field can be used (Parton and Kudryavtsev, 1988).

Further, by introducing the vector $\mathbf{U} = [u_1, u_2, u_3, \varphi]^T$ and by performing the following traditional coordinate transformation $x_1 = X_1 - vt$, $x_2 = X_2$, $x_3 = X_3$, where v is the speed of the crack tip which is assumed to move along an interface. Eqs. (1) in the moving coordinates x_1,x_2, x_3 attain the following form:

$$\mathbf{QU}_{,11} + (\mathbf{R} + \mathbf{R}^T)\mathbf{U}_{,13} + \mathbf{TU}_{,33} = 0, \tag{3}$$

where

$$\mathbf{Q} = \begin{bmatrix} Q_0 & e_{11} \\ e_{11}^T & -\varepsilon_{11} \end{bmatrix}, \quad \mathbf{R} = \begin{bmatrix} R_0 & e_{31} \\ e_{13}^T & -\varepsilon_{13} \end{bmatrix}, \quad \mathbf{T} = \begin{bmatrix} T_0 & e_{33} \\ e_{33}^T & -\varepsilon_{33} \end{bmatrix}, \tag{4}$$

$$(Q_0)_{ik} = c_{i1k1} - \rho v^2\delta_{ik}, \quad (R_0)_{ik} = c_{i1k3}, \quad (T_0)_{ik} = c_{i3k3}, \quad e_{ik} = [e_{i1k}, e_{i2k}, e_{i3k}], \tag{5}$$

δ_{ik} is the Kronecker delta and the superscript T stands for the transposed matrix.

It is assumed that the crack speed v is lower than c_{cr}, where c_{cr} is the minimum Rayleigh or Bleustein (1968)–Gulyaev (1969) wave speed for the bimaterial interface (it will be called critical surface wave speed), i.e. the subsonic regime is investigated. In this case the obtained Eq. (3) represents a set of homogeneous partial differential equations of the elliptic type (Herrmann and Noe, 1995), and therefore, the Lekhnitskii–Eshelby–Stroh method of generalized complex potentials can be applied for their solution. Assuming all fields are independent of the coordinate x_3 the required solution of the system (3) is presented in the form

$$\mathbf{U} = \mathbf{a}\mathbf{f}(z), \tag{6}$$

where $\mathbf{f}(z) = [f_1(z), f_2(z), f_3(z), f_4(z)]$ is an arbitrary 4-components vector function of the complex variable $z = x_1 + px_3$ and the vector $\mathbf{a} = [a_1, a_2, a_3, a_4]^{\mathrm{T}}$ can be found from the system

$$[\mathbf{Q} + p(\mathbf{R} + \mathbf{R}^{\mathrm{T}}) + p^2\mathbf{T}]\mathbf{a} = 0, \tag{7}$$

which can be obtained by means of the substitution of the ansatz (6) into Eq. (3). A nontrivial solution of Eq. (7) exists if p is a root of the equation

$$\det[\mathbf{Q} + (\mathbf{R} + \mathbf{R}^{\mathrm{T}})p + \mathbf{T}p^2] = 0. \tag{8}$$

It was shown that Eq. (8) has no real roots provided $v < c_{\mathrm{cr}}$, therefore we denote the roots of Eq. (8) with positive imaginary parts as p_i and the associated eigenvectors of (7) as $\mathbf{a}_i$ $(i = 1, 2, 3, 4)$. According to Suo et al. (1992) the most general real solution of Eq. (3) can be presented as

$$\mathbf{V} = \mathbf{A}\mathbf{f}(z) + \overline{\mathbf{A}\mathbf{f}}(\bar{z}), \tag{9}$$

where $\mathbf{A} = [\mathbf{a}_1, \mathbf{a}_2, \mathbf{a}_3, \mathbf{a}_4]$ is a matrix composed of eigenvectors, $\mathbf{f}(z) = [f_1(z_1), f_2(z_2), f_3(z_3), f_4(z_4)]^{\mathrm{T}}$ is an arbitrary vector function, $z_i = x_1 + p_i x_3$ $(i = 1, 2, 3, 4)$ and the overbar stands for the complex conjugate.

Comparing Eqs. (3), (6)–(9) with the associated equations of Section 2 of the paper by Herrmann and Loboda (2000) dealing with a stationary crack it can be clearly seen that formally they are the same if $(Q_0)_{ik}$, $(R_0)_{ik}$ and $(T_0)_{ik}$ from Eq. (5) are substituted instead of Q_{JK}, R_{JK} and T_{JK}, respectively, of the mentioned paper. This fact is not new and it has been mentioned in many papers. However, it means that the method developed in the paper by Herrmann and Loboda (2000) for a static interface crack in a piezoelectric bimaterial can be applied also to the investigation of a moving crack for the same dissimilar material.

3. Formulation of the problem and derivation of the basic relations

A tunnel interface crack $c \leqslant x_1 \leqslant b$, $x_3 = 0$ (Fig. 1) between two semi-infinite ceramic spaces $x_3 > 0$ and $x_3 < 0$ which are poled in the x_3-direction is considered. The material properties are defined by the matrices $c_{ijkl}^{(1)}$, $e_{lij}^{(1)}$, $\varepsilon_{ij}^{(1)}$ (for $x_3 < 0$) and $c_{ijkl}^{(2)}$, $e_{lij}^{(2)}$, $\varepsilon_{ij}^{(2)}$ (for $x_3 < 0$). It is assumed that the direction of the polarization of both materials is orthogonal to the crack front and for the upper one (upper index (1)) it can be arbitrarily oriented with respect to the crack surface (angle β) whilst for the lower one (index (2)) it is orthogonal to this surface. The crack is loaded by the concentrated loading (P_1, P_2) applied to its faces which is independent on the coordinate x_2. It is assumed as well that the crack and the loading are extending with the speed v, lower than the critical wave speed c_{cr}, in the x_1-direction and a frictionless contact zone (a, b) of the arbitrary length appears at the right crack tip.

Assuming that the coordinate system (x_1, x_3) moves together with the crack tip the interface conditions in this coordinate system can be written in the following form:

$$[u_1] = [u_2] = [u_3] = 0; \quad [\varphi] = 0; \quad [\sigma_{13}] = [\sigma_{23}] = [\sigma_{33}] = 0 \qquad \text{for } x_1 \notin (c, b), \tag{10}$$

$$\sigma_{13}^{\pm} = P_1\delta(x_1 - d); \quad \sigma_{33}^{\pm} = P_3\delta(x_1 - d); \quad \sigma_{23}^{\pm} = 0; \quad [\varphi] = 0; \quad [D_3] = 0 \qquad \text{for } x_1 \in (c, a), \tag{11}$$

$$\sigma_{13}^{\pm} = \sigma_{23}^{\pm} = 0; \quad [\sigma_{33}] = 0; \quad [u_3] = 0; \quad [\varphi] = 0; \quad [D_3] = 0 \qquad \text{for } x_1 \in (a, b), \tag{12}$$

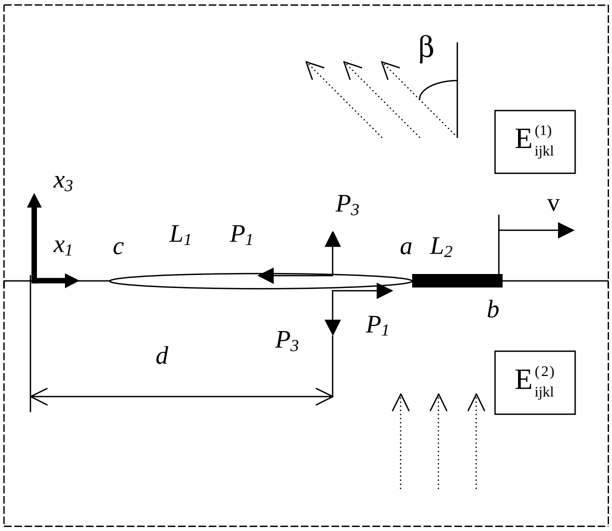

Fig. 1. Moving interface crack of a finite length in a piezoelectric bimaterial space under the action of a concentrated loading at its faces.

where $[f]=f^+-f^-$ means the jump of the function f through the material interface and $f^{\pm}(x_1)=f(x_1\pm \mathrm{i}\cdot 0)$.

Applying the approach presented for a the stationary crack by Herrmann and Loboda (2000) to the considered case of a moving crack one arrives at the following expressions written in the moving coordinate system:

$$[\mathbf{U}'(x_1)] = \mathbf{W}^+(x_1) - \mathbf{W}^-(x_1), \tag{13a}$$

$$\mathbf{t}^{(1)}(x_1,0) = \mathbf{G}\mathbf{W}^+(x_1) - \overline{\mathbf{G}}\mathbf{W}^-(x_1), \tag{13b}$$

$$[\mathbf{U}'(x_1)] = \mathbf{U}'^{(1)}(x_1,0) - \mathbf{U}'^{(2)}(x_1,0), \quad \mathbf{G} = \mathbf{B}^{(1)}\mathbf{D}^{-1}, \tag{14}$$

$$\mathbf{B} = \mathbf{R}^{\mathrm{T}} + \mathbf{T}\mathbf{A}\,\mathrm{diag}[p_1,p_2,p_3,p_4],\ \mathbf{D} = \mathbf{A}^{(1)} - \overline{\mathbf{L}}\mathbf{B}^{(1)}, \quad \mathbf{L} = \mathbf{A}^{(2)}(\mathbf{B}^{(2)})^{-1}, \tag{15}$$

$$\mathbf{W}^{\pm}(x_1) = \mathbf{W}(x_1 \pm \mathrm{i}0), \quad \mathbf{t} = [\sigma_{13},\sigma_{23},\sigma_{33},D_3]^{\mathrm{T}}, \tag{16}$$

where the vector function $W(z)$ is analytic in the whole plane with a cut along the crack region (c,b) and the superscripts (1) and (2) define the upper and lower materials, respectively.

For the accepted kind of polarization the matrix $\mathbf{G}$ has the following structure:

$$\mathbf{G} = \begin{bmatrix} \mathrm{i}g_{11} & 0 & g_{13} & g_{14} \\ 0 & \mathrm{i}g_{22} & 0 & 0 \\ g_{31} & 0 & \mathrm{i}g_{33} & g_{34} \\ g_{41} & 0 & g_{43} & \mathrm{i}g_{44} \end{bmatrix}, \tag{17}$$

where g_{11}, g_{22}, g_{33}, g_{44} are real, g_{ij} $(i,j=1,2,3,4;\ i\neq j)$ are complex, and $g_{ij}=-\bar{g}_{ji}$, $\mathrm{i}=\sqrt{-1}$.

The analysis of the matrix (17) shows that the stress–strain state in this case can be decoupled into an in-plane and an out-of-plane problem. Because the out-of-plane problem is relatively simple the main attention will be devoted to the in-plane problem which is characterized by the displacements u_1,u_3 and the electrical potential φ.

Due to the continuity of the electrical conditions at the whole interface and the absence of any electromechanical loading at infinity $W_4(z) = 0$ is valid in the whole plane. Therefore, from the matrix equation (13b) the expressions for $\sigma_{13}^{(1)}$, $\sigma_{33}^{(1)}$, $D_3^{(1)}$ at the interface can be written in the form

$$\sigma_{13}^{(1)}(x_1,0) = \mathrm{i}g_{11}W_1^+(x_1) + g_{13}W_3^+(x_1) + \mathrm{i}g_{11}W_1^-(x_1) - \bar{g}_{13}W_3^-(x_1), \tag{18}$$

$$\sigma_{33}^{(1)}(x_1,0) = g_{31}W_1^+(x_1) + \mathrm{i}g_{33}W_3^+(x_1) - \bar{g}_{31}W_1^-(x_1) + \mathrm{i}g_{33}W_3^-(x_1), \tag{19}$$

$$D_3^{(1)}(x_1,0) = g_{41}W_1^+(x_1) + g_{43}W_3^+(x_1) - \bar{g}_{41}W_1^-(x_1) - \bar{g}_{43}W_3^-(x_1). \tag{20}$$

By combining Eqs. (18) and (19) one obtains the following expressions at the interface:

$$\sigma_{33}^{(1)}(x_1,0) + \mathrm{i}m_j\sigma_{13}^{(1)}(x_1,0) = T_j[F_j^+(x_1) + \gamma_jF_j^-(x_1)], \quad j = 1,2, \tag{21}$$

where $F_j(z) = W_1(z) + \mathrm{i}S_jW_3(z)$ and the constants m_j, S_j, T_j, γ_j can be found by the following formulas:

$$m_{1,2} = \frac{(g_{13}+g_{31}) \pm \sqrt{(g_{13}+g_{31})^2 + 4g_{33}g_{11}}}{2g_{11}}, \tag{22}$$

$$T_j = g_{31} - g_{11}m_j, \quad S_j = \frac{g_{33}+m_jg_{13}}{g_{31}-m_jg_{11}}, \quad \gamma_j = \frac{g_{12}-m_jg_{11}}{T_j}, \qquad j = 1,2. \tag{23}$$

As it follows from the analysis of the formulas (22) and (23) the constants $m_{1,2}$, $S_{1,2}$ are complex while $T_{1,2}$, $\gamma_{1,2}$ are real. Besides the following relations

$$S_{1,2} = -m_{1,2}, \quad \gamma_1 = 1/\gamma_2 \tag{24}$$

hold true.

Using Eq. (13a) leads to the following expression for the derivatives of the displacement jumps:

$$[u_1'(x_1)] + \mathrm{i}S_j[u_3'(x_1)] = F_j^+(x_1) - F_j^-(x_1), \quad j = 1,2. \tag{25}$$

In the following the attention will be paid to the case of $j = 1$ only because the results for $j = 2$ can be found from the results for this case.

4. Moving crack of a finite length

The substitution of the presentations (21) and (25) in the boundary conditions (10)–(12) leads to the following inhomogeneous combined Dirichlet–Riemann problem with respect to the function $F_1(z)$

$$F_1^+(x_1) + \gamma_1F_1^-(x_1) = T_1^{-1}g(x_1) \quad \text{for } x_1 \in (c,a), \tag{26}$$

$$\mathrm{Im}F_1^{\pm}(x_1) = 0 \quad \text{for } x_1 \in (a,b), \tag{27}$$

where $g(x_1) = (P_3 + \mathrm{i}m_1P_1)\delta(x_1 - d)$.

The solution of problems (26) and (27) for trivial values of $F(z)$ at infinity is presented in the paper by Herrmann et al. (2004) and has the following form:

$$F_1(z) = \frac{X_2(z)}{d-z}\left[\mathrm{Re}(I_0) + \mathrm{i}\mathrm{Im}(I_0)\frac{Y(z)}{Y(d)}\right], \tag{28}$$

where

$$X_2(z) = \mathrm{e}^{\mathrm{i}\varphi(z)}/\sqrt{(z-c)(z-a)}, \tag{29}$$

$$\varphi(z) = 2\varepsilon_1 \ln \frac{\sqrt{(b-a)(z-c)}}{\sqrt{l(z-a)} + \sqrt{(a-c)(z-b)}}, \quad \varepsilon_1 = \frac{\ln \gamma_1}{2\pi}, \tag{30}$$

$$Y(z) = \sqrt{(z-a)/(z-b)}, \quad I_0 = \frac{1}{2\pi \mathrm{i}} \frac{P_3 + \mathrm{i}m_1 P_1}{T_1 X_2^+(d)}. \tag{31}$$

Using the obtained solution and the formula (25) leads to the following expressions for the derivatives of the displacement jumps for $x_1 \in (c,a)$:

$$[u_1'(x_1,0)] + \mathrm{i}S_1[u_3'(x_1,0)] = \frac{(\gamma_1+1)}{\gamma_1} \frac{X_2(x_1)}{d-x_1} \left[\mathrm{Re}(I_0) + \mathrm{i}\mathrm{Im}(I_0) \frac{Y(x_1)}{Y(d)} \right]. \tag{32}$$

Similarly it follows from Eqs. (21) and (28) that in the contact zone (a,b)

$$\begin{aligned} \sigma_{33}^{(1)}(x_1,0) = & -\frac{r_1 \mathrm{Re}(I_0)}{(x_1-d)} \left(\cosh \varphi_2(x_1) + \frac{1-\gamma_1}{1+\gamma_1} \sinh \varphi_2(x_1) \right) \\ & - \frac{r_1 \mathrm{Im}(I_0)}{(x_1-d)} \left(\sinh \varphi_2(x_1) + \frac{1-\gamma_1}{1+\gamma_1} \cosh \varphi_2(x_1) \right) \frac{Y_1(x_1)}{Y(d)}, \end{aligned} \tag{33}$$

$$[u_1'(x_1,0)] = -\frac{2\cosh \varphi_2(x_1)}{(x_1-d)} \frac{Y_1(x_1)}{Y(d)} \mathrm{Im}(I_0), \tag{34}$$

while for $x_1 > b$:

$$\sigma_{33}^{(1)}(x_1,0) + \mathrm{i}m_1\sigma_{13}^{(1)}(x_1,0) = T_1(\gamma_1+1)\frac{X_2(x_1)}{d-x_1} \left[\mathrm{Re}(I_0) + \mathrm{i}\mathrm{Im}(I_0) \frac{Y(x_1)}{Y(d)} \right], \tag{35}$$

where

$$\varphi_2(x_1) = 2\varepsilon_1 \arctan \sqrt{\frac{(a-c)(b-x_1)}{(b-c)(x_1-a)}}, \quad Y_1(x_1) = \sqrt{\frac{x_1-a}{b-x_1}}, \quad r_1 = (1+\gamma_1)T_1.$$

Using the first formula (13) and the expressions (18)–(20) gives the following expression for the electrical displacement for $x_1 \in (a,b)$:

$$D_3^{(1)}(x_1,0) = \mathrm{Re}(g_{41})[u_1'(x_1,0)] + \frac{\mathrm{Im}(g_{41})\mathrm{Im}(g_{13}) - \mathrm{Im}(g_{43})g_{11}}{(\mathrm{Im}(g_{31}))^2 - g_{33}g_{11}} (\sigma_{33}^{(1)}(x_1,0) - \mathrm{Re}(g_{31})[u_1'(x_1,0)]). \tag{36}$$

Introducing the following stress and electrical intensity factors (IFs)

$$k_1 = \lim_{x_1 \to a+0} \sqrt{2\pi(x_1-a)}\sigma_{33}^{(1)}(x_1,0), \tag{37}$$

$$k_2 = \lim_{x_1 \to b+0} \sqrt{2\pi(x_1-b)}\sigma_{13}^{(1)}(x_1,0), \tag{38}$$

$$k_4 = \lim_{x_1 \to a+0} \sqrt{2\pi(x_1-a)}D_3^{(1)}(x_1,0) \tag{39}$$

and using the relations (33) and (35) leads to the following formulas for k_1 and k_2:

$$k_1 = -\sqrt{\frac{2}{\pi}}\frac{\sqrt{d-c}}{\sqrt{(a-d)(a-c)}}[(P_3 - \mathrm{Im}(m_1)P_1)\cos(\varphi_1(d)) + \mathrm{Re}(m_1)P_1\sin(\varphi_1(d))], \tag{40}$$

$$k_2 = -\frac{1+\gamma_1}{\sqrt{2\pi\gamma_1}}\frac{\sqrt{1-\theta}}{\sqrt{b-d}}\left[P_1\cos(\varphi_1(d)) - \frac{P_3 - \mathrm{Im}(m_1)P_1}{\mathrm{Re}(m_1)}\sin(\varphi_1(d))\right], \tag{41}$$

where

$$\varphi_1(d) = 2\varepsilon_1 \ln\frac{\sqrt{(b-a)(d-c)}}{\sqrt{(b-c)(a-d)}+\sqrt{(a-c)(b-d)}}, \quad \theta = \frac{b-d}{b-c}.$$

On the base of Eq. (36) the electrical IF k_4 can be expressed via the SIF k_1 in the following way:

$$k_4 = \left(\frac{\mathrm{Im}(g_{43})g_{11} - \mathrm{Im}(g_{41})\mathrm{Im}(g_{13})}{g_{33}g_{11} - (\mathrm{Im}(g_{13}))^2} + \left(\mathrm{Re}(g_{41}) + \frac{\mathrm{Re}(g_{31})(\mathrm{Im}(g_{41})\mathrm{Im}(g_{13}) - \mathrm{Im}(g_{43})g_{11})}{g_{33}g_{11} - (\mathrm{Im}(g_{13}))^2}\right)\frac{\gamma_1^2 - 1}{2\gamma_1 r_1}\right)k_1. \tag{42}$$

The obtained formulas are mathematically correct for any position of the point a; however, the obtained solution becomes physically valid if the following inequalities:

$$\sigma_{33}^{(1)}(x_1, 0) \leqslant 0 \quad \text{for } x_1 \in (a, b), \qquad [u_3(x_1, 0)] \geqslant 0 \quad \text{for } x_1 \in (c, a) \tag{43}$$

are satisfied and the contact zone model in Comninou's (1977) sense takes place. It can be shown that for the satisfaction of the mentioned inequalities it is necessary and sufficient to reach the smooth closing of the crack

$$\lim_{x_1 \to a-0} \sqrt{a - x_1}[u_3'(x_1, 0)] = 0,$$

which is equivalent to the equation $k_1 = 0$. Both of these equations due to the formulas (32) and (40) can be written in the form of the following single transcendental equation

$$\tan\varphi_1(\lambda) = -\frac{P_3 - \mathrm{Im}(m_1)P_1}{\mathrm{Re}(m_1)P_1}, \tag{44}$$

where

$$\varphi_1(\lambda) = 2\varepsilon_1 \ln\frac{\sqrt{\lambda(1-\theta)}}{\sqrt{\theta - \lambda} + \sqrt{\theta(1-\lambda)}} \tag{45}$$

and $\lambda = \frac{b-a}{b-c}$ is the relative contact zone length.

It was known earlier and is confirmed here by a numerical verification that for the satisfaction of both inequalities (43) the maximum root of Eq. (44) situated in the interval $(0, 1)$ should be chosen. This root will be designated as λ_0. In a general case Eq. (44) cannot be solved exactly and a numerical procedure should be used, but for small values of λ ($\lambda \ll 1$) the following asymptotic solution of Eq. (44)

$$\lambda_0 \approx \tilde{\lambda}_0 = \frac{4\theta}{1-\theta}\exp\left\{\frac{1}{\varepsilon_1}\left[\tan^{-1}\left(-\frac{P_3 - \mathrm{Im}(m_1)}{\mathrm{Re}(m_1)P_1}\right) + \pi n\right]\right\} \tag{46}$$

is valid and the appropriate value of n which defines the maximum λ_0 from the set (46) should be taken.

Introducing in formula (41) Eq. (44) leads to the following expression for the SIF k_2 which corresponds to the real contact zone length

$$k_2 = -\frac{1}{\mathrm{Re}(m_1)} \frac{1+\gamma_1}{\sqrt{2\pi\gamma_1(b-d)}} \sqrt{1-\theta} \sqrt{(\mathrm{Re}(m_1)P_1)^2 + (P_3 - \mathrm{Im}(m_1)P_1)^2}. \tag{47}$$

5. Moving crack of a semi-infinite length

The model of a moving crack with a finite length considered in the previous chapter is an idealization which for a crack in a homogeneous material was suggested by Yoffe (1951), and it is suitable for the investigation of local processes at the crack tip. However, together with this model it is of interest to analyze the propagating crack with a semi-infinite length which for a case of two dissimilar isotropic materials was initiated by Gol'dstein (1966). The results for this case can be obtained as a particular case of the above mentioned solution.

Thus the crack tip b will be connected with the origin of the moving coordinate system (x_1, x_3). Further, the contact zone length will be denoted as r, and the distance from the applied concentrated forces to the crack tip as d_1. It is clear that in this coordinate system $b = 0$, $a = -r$ and $d = -d_1$ hold true. Now if the left crack tip c tends to $(-\infty)$ and by performing the analysis of Eqs. (32)–(35), which is similar to that which was presented in details by Herrmann et al. (2004), the following equations can be obtained:

$$\sigma_{33}^{(1)}(x_1,0) + \mathrm{i}m_1\sigma_{13}^{(1)}(x_1,0) = \frac{R(1+\gamma_1)\exp(\mathrm{i}\varphi(x_1))}{2\pi(x_1+d_1)} \times \left[-\cos(\eta+\vartheta)\sqrt{\frac{d_1-r}{x_1+r}} + \mathrm{i}\sin(\eta+\vartheta)\sqrt{\frac{d_1}{x_1}}\right] \quad \text{for } x_1 > 0, \tag{48}$$

$$\sigma_{33}^{(1)}(x_1,0) = -\frac{R}{\pi(x_1+d_1)}\sin(\eta+\vartheta)\sinh\varphi_3(x_1)\sqrt{\frac{d_1}{-x_1}} - \frac{R}{\pi(x_1+d_1)}\cos(\eta+\vartheta)\cosh\varphi_3(x_1)\sqrt{\frac{d_1-r}{x_1+r}}, \tag{49}$$

$$[u_1'(x_1,0)] = \frac{R}{\pi T_1\sqrt{\gamma_1}(x_1+d_1)}\left[\sin(\eta+\vartheta)\sqrt{\frac{d_1}{-x_1}}\right] \quad \text{for } x_1 \in (-r,0), \tag{50}$$

$$[u_1'(x_1,0)] + \mathrm{i}m_1[u_3'(x_1,0)] = T_1R\frac{1+\gamma_1}{\gamma_1}\frac{\exp(\mathrm{i}\varphi_3(x_1))}{2\pi(x_1+d_1)} \times \left[\sin(\eta+\vartheta)\sqrt{\frac{d_1}{-x_1}} + \mathrm{i}\cos(\eta+\vartheta)\sqrt{\frac{d_1-r}{-x_1-r}}\right] \quad \text{for } x_1 < -r, \tag{51}$$

where

$$R = \sqrt{(P_3 - \mathrm{Im}(m_1)P_1)^2 + (\mathrm{Re}(m_1)P_1)^2}, \tag{52}$$

$$\varphi(z) = -2\varepsilon_1 \ln\frac{1}{i}\left(\sqrt{\frac{z}{r}} + \sqrt{1+\frac{z}{r}}\right), \quad \eta = -\arctan\frac{\mathrm{Re}(m_1)P_1}{P_3 - \mathrm{Im}(m_1)P_1}, \tag{53}$$

$$\vartheta = -2\varepsilon_1 \ln\left(\sqrt{\frac{d_1}{r} - 1} + \sqrt{\frac{d_1}{r}}\right), \quad \varphi_3(x_1) = 2\varepsilon_1 \arctan\sqrt{\frac{r+x_1}{-x_1}}. \tag{54}$$

It is worth to be mentioned that for the electrical displacement D_3 the relation (36) remains valid provided the stresses and displacements are used from the expressions (48)–(51).

On the base of the formulas (40) and (41) the SIFs can be written as

$$k_{\infty 1} = -\sqrt{\frac{2}{\pi}}\frac{R}{\sqrt{d_1 - r}}\cos(\eta + \vartheta), \tag{55}$$

$$k_{\infty 2} = -\frac{R(1+\gamma_1)}{\mathrm{Re}(m_1)\sqrt{2\pi d_1 \gamma_1}}\sin(\eta + \vartheta) \tag{56}$$

and Eq. (44) for the determination of the real contact zone length attains the following very simple form:

$$\cos(\vartheta + \eta) = 0. \tag{57}$$

It is convenient to introduce the new parameters $\alpha = \lambda/\theta$ and $\alpha_\infty = r/d_1$ which define the coefficients of the contact zone length and the distance from the concentrated force to the crack tip for cracks of finite and infinite lengths, respectively. Therefore the exact solution of Eq. (57) can be given as follows

$$\alpha_\infty = \cosh^{-2}\left[\frac{1}{2\varepsilon_1}(\eta + \pi(0.5 - n))\right], \tag{58}$$

where the integer n should be taken similarly to the previous case.

Further, the SIF k_2 at the tip of a crack with semi-infinite length can be written in the form

$$k_{\infty 2} = -\frac{R(\gamma_1 + 1)}{\mathrm{Re}(m_1)\sqrt{2\pi d_1 \gamma_1}}. \tag{59}$$

For the comparison of the results of the above two models consider Eq. (58) for small values of α_∞ ($\alpha_\infty \ll 1$). In this case the approximate equality $\cosh^2(x) \approx 0.25\exp(2x)$ is valid and we arrive at the following asymptotic formula for α_∞:

$$\alpha_\infty \approx \tilde{\alpha}_\infty = 4\exp\left[-\frac{1}{\varepsilon_1}(\eta + \pi(0.5 - n))\right]. \tag{60}$$

A comparable analysis of Eqs. (46), (47) and (59), (60) shows the validity of the following equations:

$$\tilde{\alpha}_\infty = (1-\theta)\tilde{\alpha}_0, \quad k_{\infty 2} = (1-\theta)^{-1}k_2. \tag{61}$$

6. Numerical results and discussion for an electrically permeable crack

The numerical analysis has been performed for a bimaterial composed of piezoceramics PZT4 (the upper material) and PZT5 (the lower one) with the material properties shown in Table 1. The position of the concentrated loading at the crack faces was defined by the value $\theta =$ 0.2 and the transverse component of the loading was used to be zero ($P_1/P_3 = 0$).

In Figs. 2–5 the dependencies of the parameters ε_1, α, $\tilde{k}_2 = \frac{k_2}{P_3}\sqrt{b-d}$ from the crack speed are presented. The solid lines correspond to a crack of a finite length and the dashed lines are related to the crack of a semi-infinite length. Particularly in Fig. 2 the variation of the oscillation index ε_1 with respect to the crack speed v for different directions of polarization of the upper materials defined by the angle β are shown. Line I correspond to $\beta = 0$ and the line II is given for $\beta = \pi/6$. The values of the critical speed

Table 1
Material properties

Material constants	PZT-5	PZT-4
c_{11} (N/m^2)	10.3×10^{10}	13.9×10^{10}
c_{33} (N/m^2)	10.2×10^{10}	11.5×10^{10}
c_{12} (N/m^2)	5.8×10^{10}	7.78×10^{10}
c_{13} (N/m^2)	5.9×10^{10}	7.43×10^{10}
c_{44} (N/m^2)	2.5×10^{10}	2.56×10^{10}
c_{66} (N/m^2)	2.25×10^{10}	3.06×10^{10}
e_{31} (C/m^2)	−7.78	−5.2
e_{15} (C/m^2)	12.9	12.7
e_{33} (C/m^2)	15.2	15.1
ε_{11} (C/V m)	8.92×10^{-9}	6.45×10^{-9}
ε_{33} (C/V m)	7.93×10^{-9}	5.62×10^{-9}
ρ (kg/m^3)	7600	7500

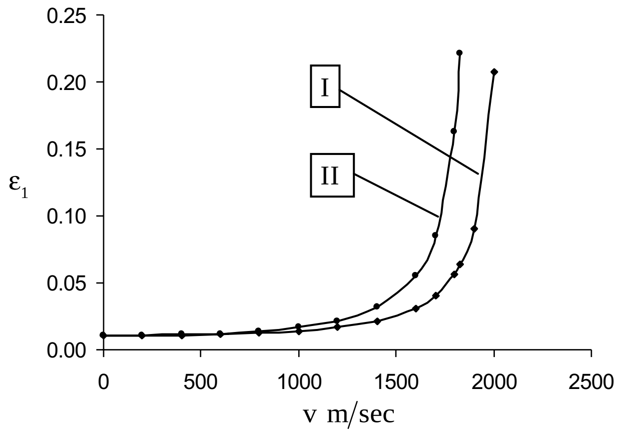

Fig. 2. The variation of the oscillation index ε_1 with respect to the crack speed v for different directions of polarization of the upper materials.

for these cases are equal to 1975.59 m/s and 1817.76 m/s, respectively. In Figs. 3 and 4 the variation of the relative contact zone length α with respect to v for different directions of polarization defined by $\beta = 0$ (line I), $\beta = \pi/3$ (II) and $\beta = \pi$ (III) are shown. Because of the smallness of the contact zone length for small and moderate values of v the results in Fig. 3 are given in a logarithmic scale and the difference between the results for cracks with finite or semi-infinite lengths is not visible in this case. The results in Fig. 4 are presented for a crack speed v tending to the critical speed c_{cr} and in Fig. 5 the variation of the dimensionless SIF $\tilde{k}_2$ for the full range of v in the interval $(0, c_{cr})$ for $\beta = 0$ (line I) and $\beta = \pi$ (II) are presented.

It follows from the analysis of the results presented in Figs. 2–5 that all values essentially depend on the crack speed v especially for the near-critical speed region. Particularly for this region the value of the relative contact zone length α tends to the value of θ for $v \to c_{cr}$ and the SIF k_2 grows to infinity. It is clear as well that the investigated parameters do not depend essentially from the variation of the direction of polarization of the upper material and, moreover, the results for cracks with finite or infinite lengths, respectively differ only inconsiderable. This conclusion confirms the possibility for using interface crack models with finite or semi-infinite crack lengths for the investigation of local effects at the correspondent crack tips.

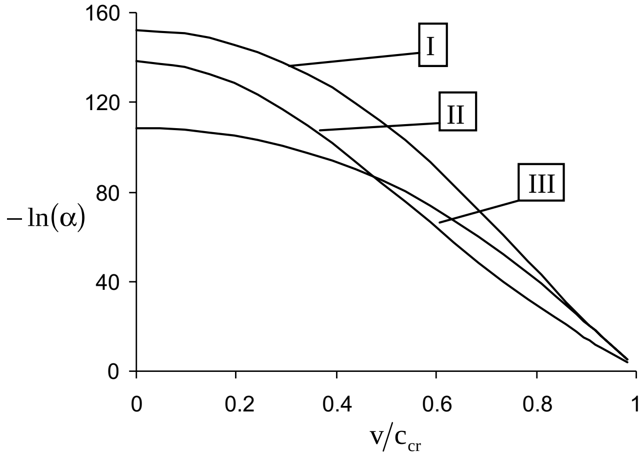

Fig. 3. The variation of the relative contact zone length α with respect to v for the directions of polarization defined by $\beta = 0$ (line I), $\beta = \pi/3$ (II) and $\beta = \pi$ (III).

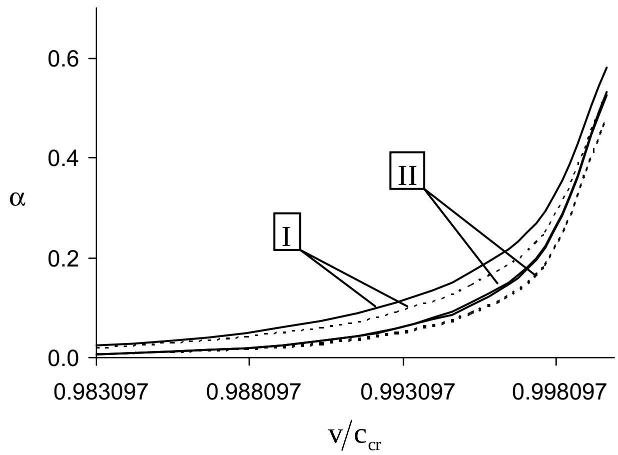

Fig. 4. The variation of the relative contact zone length α with respect to v for near critical wave speeds.

7. Electrically impermeable crack

Let us consider now the case of an electrically impermeable crack. It was mentioned in many papers (see for example the review given by Herrmann et al., 2001) that the electrically permeable assumption is more realistic than the impermeable one. However, this assumption can be useful in some cases (Suo et al., 1992), for example if an electrical charge is prescribed at the crack faces.

The formulation of the problem is the same as earlier except that the open part of the crack is now assumed electrically insulated, and the concentrated electrical charge with the intensity D is prescribed at the points $(e, 0)$ of the crack faces (Fig. 6). Because it was shown above that the direction of polarization has no essential influence onto the parameters in question these directions here are chosen co-directed with the axis x_3. The conditions at the material interface in the moving coordinates (x_1, x_3) introduced in Section 2 with taking into account in-plane components only can be written as follows:

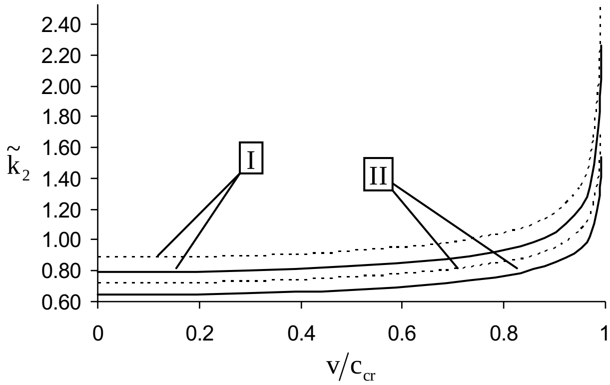

Fig. 5. The variation of the dimensionless SIF $\tilde{k}_2$ with respect to v for $\beta = 0$ (line I) and $\beta = \pi$ (II).

$$[\mathbf{U}] = 0, \quad [\mathbf{t}] = 0 \qquad \text{for } x_1 \notin (c, b), \tag{62a}$$

$$\sigma_{13}^{\pm} = P_1\delta(x_1 - d), \quad \sigma_{33}^{\pm} = P_3\delta(x_1 - d), \quad D_3 = D\delta(x_1 - e) \qquad \text{for } x_1 \in (c, a), \tag{62b}$$

$$\sigma_{13}^{\pm} = 0, \quad [\sigma_{33}] = 0, \quad [u_3] = 0, \quad [\varphi] = 0, \quad [D_3] = 0 \qquad \text{for } x_1 \in (a, b). \tag{62c}$$

Following the analysis presented in Section 2 and taking into account the analytical manipulations performed by Herrmann et al. (2001) leads to the following expressions for the stresses, electrical displacement as well as for the derivatives of the mechanical displacements and electrical potential jumps at the interface in the moving coordinate system

$$\sigma_{33}^{(1)}(x_1, 0) + m_{j4}D_3^{(1)}(x_1, 0) + \mathrm{i}m_{j1}\sigma_{13}^{(1)}(x_1, 0) = F_j^{+}(x_1) + \gamma_j F_j^{-}(x_1), \quad j = 1, 3, 4, \tag{63}$$

$$n_{j1}[u_1'(x_1, 0)] + \mathrm{i}(n_{j3}[u_3'(x_1, 0)] + n_{j4}[\varphi'(x_1, 0)]) = F_j^{+}(x_1) - F_j^{-}(x_1), \quad j = 1, 3, 4, \tag{64}$$

where $F_j(z)$ are functions analytical in the whole plane with a cut along the crack, $m_{j4} = S_{j4}$, $m_{j1} = -\mathrm{i}S_{j1}$, $n_{j1} = Y_{j1}$, $n_{j3} = -\mathrm{i}\,Y_{j3}$, $n_{j4} = -\mathrm{i}\,Y_{j4}$ depend on the crack speed v and are real values, $\mathbf{Y}_j = [Y_{j1},\ Y_{j3},\ Y_{j4}] = \mathbf{S}_j\,\mathbf{G}$ and γ_j and $\mathbf{S}_j^{\mathrm{T}} = [S_{j1}, S_{j3}, S_{j4}]^{\mathrm{T}}$ are the eigenvalues and the eigenvectors of the system

$$(\gamma\mathbf{G}^{\mathrm{T}} + \overline{\mathbf{G}}^{\mathrm{T}})\mathbf{S}^{\mathrm{T}} = 0. \tag{65}$$

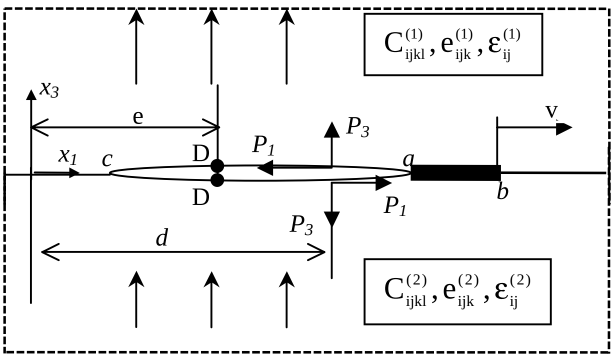

Fig. 6. Geometry of the problem and the distribution of an electromechanical loading for the case of an electrically insulated crack.

It should be mentioned that the above conclusion concerning the reality of the coefficients m_{j1}, m_{j4}, n_{j1}, n_{j3} and n_{j4} is valid provided γ_j are real, however, the last condition is satisfied for a variety of practically used bimaterial combinations.

The substitution of Eqs. (63), (64) into the interface conditions (62) leads to the following combined Dirichlet–Riemann problems for the functions $F_j(z)$, $j = 1, 3$:

$$F_j^+(x_1) + \gamma_j F_j^-(x_1) = (P_3 + \mathrm{i}m_{j1}P_1)\delta(x_1 - d) + m_{j4}D\delta(x_1 - e) \quad \text{for } x_1 \in (c, a), \tag{66}$$

$$\mathrm{Im}F_j^{\pm}(x_1) = 0 \quad \text{for } x_1 \in (a, b) \tag{67}$$

and to the Hilbert problem for the function $F_4(z)$

$$F_4^+(x_1) + F_4^-(x_1) = (P_3 + \mathrm{i}m_{41}P_1)\delta(x_1 - d) + m_{44}D\delta(x_1 - e) \quad \text{for } x_1 \in (c, a). \tag{68}$$

It is proved analytically that $\gamma_1 = 1/\gamma_3$, $m_{14} = m_{34}$, $m_{11} = -m_{31}$ and therefore, the solution of the problem (66), (67) for $j = 3$ can be found from the solution of this problem for $j = 1$. This solution is found in the same way as for the combined Dirichlet–Riemann problem (26), (27) and for trivial values of $F_1(z)$ at infinity has the following form

$$F_1(z) = \frac{X_2(z)}{2\pi\sqrt{\gamma_1}}\left[\left(\Psi_1 + \mathrm{i}\Psi_2\frac{Y(z)}{Y(d)}\right)\frac{\sqrt{(d-c)(a-d)}}{(d-z)} + \left(\Psi_3 + \mathrm{i}\Psi_4\frac{Y(z)}{Y(e)}\right)\frac{\sqrt{(e-c)(a-e)}}{(e-z)}\right], \tag{69}$$

where

$$\Psi_1 = P_3\cos\varphi_1(d) + m_{11}P_1\sin\varphi_1(d), \quad \Psi_2 = m_{11}P_1\cos\varphi_1(d) - P_3\sin\varphi_1(d), \tag{70}$$

$$\Psi_3 = m_{14}D\cos\varphi_1(e), \quad \Psi_4 = -m_{14}D\sin\varphi_1(e), \tag{71}$$

whilst $X_2(z)$, $\varphi(z)$ and $Y(z)$ are defined by the formulas (29)–(31), respectively.

The solution of the problem (68) under the trivial condition at infinity reads follows (Muskhelishvili, 1977):

$$F_4(z) = \frac{X_0(z)}{2\pi\mathrm{i}}\left[\frac{P_3 + \mathrm{i}m_{41}P_1}{X_0^+(d)(d-z)} + \frac{m_{44}D}{X_0^+(e)(e-z)}\right], \tag{72}$$

where $X_0(z) = [(z - c)(z - a)]^{-1/2}$.

Using the obtained solutions and the formulas (63), (64) the expressions for the mechanical stresses, electrical displacements as well as for the derivatives of the mechanical displacements and electrical potential jumps at the interface are found and presented in Appendix A. Eqs. (A.2a), (A.2b) and (A.3a), (A.3b) can be considered as a system of linear algebraic equations from which $\sigma_{33}^{(1)}(x_1, 0)$, $D_3^{(1)}(x_1, 0)$ for $x_1 \in (a, b)$ and $[u_3'(x_1, 0)]$, $[\varphi'(x_1,0)]$ for $x_1 \in (a, b)$ can be easily calculated.

The introduction of the stress and electrical intensity factors defined by the formulas (37)–(39) and the use of Eqs. (B.1) and (B.2) lead to the following expressions for the required IFs

$$k_1 = \frac{\sqrt{2}}{\sqrt{\pi}(m_{44} - m_{14})}\left(\sqrt{\frac{d-c}{(a-c)(a-d)}}(m_{14}P_3 - m_{44}\Psi_1) + \sqrt{\frac{e-c}{(a-c)(a-e)}}(m_{44}m_{14}D - m_{44}\Psi_3)\right), \tag{73}$$

$$k_2 = -\frac{(1+\gamma_1)}{m_{11}\sqrt{2\pi\gamma_1}}\left(\Psi_2\sqrt{\frac{d-c}{(b-c)(b-d)}} + \Psi_4\sqrt{\frac{e-c}{(b-c)(b-e)}}\right). \tag{74}$$

$$k_4 = \frac{\sqrt{2}}{\sqrt{\pi}(m_{14} - m_{44})}\left(\sqrt{\frac{d-c}{(a-c)(a-d)}}(P_3 - \Psi_1) + \sqrt{\frac{e-c}{(a-c)(a-e)}}(m_{44}D - \Psi_3)\right). \tag{75}$$

The obtained solution is valid for any position of the point a, however, to make it physically correct the inequalities (43) should be satisfied. The satisfaction of the mentioned inequalities is not so clear as in the case of an electrically permeable crack. First of all we formulate the following equations:

$$k_1 = 0 \tag{76a}$$

and $\sqrt{a - x_1}[u_3'(x_1, 0)] = 0$ which can be written in the form

$$\Theta_{11}k_1 + \Theta_{14}k_4 = 0, \tag{76b}$$

where $\Theta_{11} = (n_{44}\sqrt{\alpha/\gamma_1} - n_{14})/\Delta_n$; $\Theta_{14} = (m_{14}n_{44}\sqrt{\alpha/\gamma_1} - m_{44}n_{14})/\Delta_n$, $\Delta_n = n_{13}n_{44} - n_{43}n_{14}$, $\alpha = \frac{(\gamma_1+1)^2}{4\gamma_1}$.

The maximum roots from the interval $(0, 1)$ of Eqs. (76a) and (76b) generally can be found numerically, and they are designated by λ_1 and λ_2, respectively. However, for small values of these parameters the following asymptotic formulas are valid

$$\widetilde{\lambda}_1 = \exp\left[\frac{1}{\varepsilon_1}\left((-1)^n\left(\arcsin\left(\frac{\Delta_1}{\Delta_{pd}}\right) - \arcsin\left(\frac{m_{14}}{\Delta_{pd}m_{44}}(\Theta_1 m_{44}D + P_3)\right)\right) + \pi n\right)\right], \tag{77a}$$

$$\widetilde{\lambda}_2 = \exp\left[\frac{1}{\varepsilon_1}\left((-1)^n\left(\arcsin\left(\frac{\Delta_1}{\Delta_{pd}}\right) - \arcsin\left(\frac{(\Theta_{11}m_{14} - \Theta_{14})}{\Delta_{pd}(m_{44}\Theta_{11} - \Theta_{14})}(\Theta_1 m_{44}D + P_3)\right)\right) + \pi n\right)\right], \tag{77b}$$

where

$$\Delta_{pd} = \sqrt{\Delta_x^2 + \Delta_y^2},\ \Delta_x = m_{11}P_1\cos U - \Theta_1 m_{14}D\sin V - P_3\sin U,$$
$$\Delta_y = \Theta_1 m_{14}D\cos V + P_3\cos U + m_{11}P_1\sin U,$$
$$\Theta_1 = \sqrt{\frac{(1-\vartheta)\theta}{(1-\theta)\vartheta}},\ \theta = \frac{b-d}{b-c},\ \vartheta = \frac{b-e}{b-c},\ U = \varepsilon_1\ln\frac{1-\theta}{4\theta},\ V = \varepsilon_1\ln\frac{1-\vartheta}{4\vartheta}.$$

The numerical analysis showed that in the considered case the inequalities (43) are satisfied not only for a single value of the contact zone length λ, but usually for a set of positions $a \in [a_1, a_2]$, where $a = b - \lambda l$, $a_1 = b - \lambda_1 l$, $a_2 = b - \lambda_2 l$ and l is the crack length. In other terms this set can be defined as follows

$$\Omega_a = [a \geqslant a_1 \cap a \leqslant a_2]. \tag{78}$$

This situation is not traditional because usually the real position of the point a is uniquely defined by the inequalities (43). It was already mentioned and analyzed by Herrmann et al. (2001) and Herrmann and Loboda (2003) concerning a stationary crack. We only mention here that the existence and the size of the set Ω_a essentially depend on the materials, the electromechanical loading and the crack speed. This set exists only if $a_1 \leqslant a_2$; for $a_2 = a_1$ arises the unique point satisfying both inequalities (43) and for $a_2 < a_1$ follows $\Omega_a = \emptyset$, and the contact zone model defined by the boundary conditions (62) does not exist. In the last case more realistic conditions should be used.

The analysis shows that the most characteristic situation is connected with $\Omega_a \neq \emptyset$, and it is clear that for any of such cases a unique contact zone defined by a real position of the point a should exist. In the paper by Herrmann et al. (2001) a position in question has been defined by means of the theorem of the minimum potential energy. The same analysis remains valid here and, therefore, the real position of the point a coincides with a_1 provided $\Omega_a \neq \emptyset$ holds true.

The numerical analysis gives a rather manifold picture of results for the case of an electrically impermeable crack. But the main conclusions noticed for a stationary crack remain valid here. Particularly, for

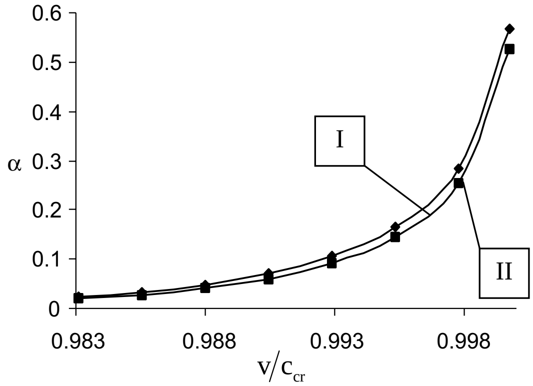

Fig. 7. Dependencies of α for finite and semi-infinite cracks with respect to v tending to c_{cr} for the case of electrically impermeable crack-face conditions.

$D = 0$ the set Ω_a usually exists and is not empty. An increase of D leads to a decrease of $(a_2 - a_1)$ till to the point where $a_2 = a_1$. In this point $\Omega_a = a_2 = a_1$ holds true, and the further increasing of D gives $\Omega_a = \emptyset$ and the contact zone model does not exist. On the other hand decrease of D leads to the decrease of both values a_1 and a_2, but their difference increases. Concerning the influence of the crack tip speed it is worth to be mentioned that an increase of v usually decreases the difference $(a_2 - a_1)$ and in some cases leads to a transformation from $\Omega_a = \emptyset$ to the opposite situation.

In Fig. 7 for the same bimaterial as in Table 1 the dependence of the relative contact zone length α with respect to the crack tip speed in the near-critical speed region is presented. Line I corresponds to a finite crack and line II to a semi-infinite one. The mechanical loading was the same as for the electrically permeable crack ($P_1 = 0, P_3 = -10^6$ N/m), but in addition an electrical charge of intensity $D = -2.48 \times 10^{-4}$ C/m^2 was prescribed in the point $(0, e)$ with $(b - e)/(b - c)^{-1} = 0.15$. It follows from the presented figures that the behavior is similar to the case of an electrically permeable crack, i.e. the increase of v leads to an essential increase of the contact zone length especially in the near-critical speed zone.

8. Conclusion

A moving interface crack with a mechanically frictionless and electrically permeable contact zone at the leading crack tip in a piezoelectric bimaterial is considered. In the first chapters of the paper the open part of the crack is assumed to be electrically permeable and concentrated forces of an arbitrary direction are prescribed at the crack faces.

By introduction of a moving coordinate system attached to the crack tip and by using the formal identity of the obtained relations to the associated case of a stationary crack the presentations of the mechanical displacements and electrical potential jumps (13a) as well as of the stresses and electrical displacements (13b) at the material interface via a sectionally holomorphic vector-function are obtained.

A finite length interface crack (Yoffe-type crack) is considered in Section 4. By means of the presentations (13) this problem is reduced to an inhomogeneous combined Dirichlet–Riemann problems (26) and (27) which has been solved exactly. All electromechanical characteristics at the interface are presented in a closed form for an arbitrary contact zone length. Further, from the additional inequalities (43) the transcendental equation (44) for the determination of the real contact zone length and the formula (47) for the associated stress intensity factors of the shear stress are obtained. As a particular case of the obtained solution a semi-infinite interface crack is considered in Section 5 and simple formulas (58), (59) for the contact zone length and the stress intensity factor of the shear stress are given.

The numerical illustrations of the obtained solutions for an electrically permeable crack are presented for the bimaterial PZT4/PZT5 (Table 1) in Figs. 2–5. In all considered cases an essential increase of the bimaterial constant ϵ, the real contact zone length and the associated shear stress intensity factor for a crack speed v tending to the critical (Rayleigh or Bleustein–Gulyaev) wave speed is observed.

The case of electrically impermeable crack faces is considered briefly in Section 7. In this case in addition to the Dirichlet–Riemann problem (67) the Hilbert problem (68) arises. However, an exact analytical solution has been obtained in this case as well and the prescribed concentrated electrical charge (in addition to the mechanical loading) at the crack faces is taken into account.

Acknowledgment

One of the authors (V.L.) gratefully acknowledges a grant from the German Academic Research Service (DAAD).

Appendix A

The expressions for the mechanical stresses, electrical displacement, the derivatives of the mechanical displacements and electrical potential jumps at the interface for an electrically impermeable crack

$$\sigma_{13}^{(1)}(x_1,0) = -\frac{(1+\gamma_1)}{m_{11}\sqrt{(x_1-c)\gamma_1}2\pi}\left(\left(\Psi_1\frac{\sqrt{d-c}}{x_1-d}+\Psi_3\frac{\sqrt{e-c}}{x_1-e}\right)\sin\varphi(x_1)\right.$$
$$\left.+\left(\Psi_2\frac{\sqrt{(b-d)(d-c)}}{\sqrt{x_1-b}(x_1-d)}+\Psi_4\frac{\sqrt{(e-d)(e-c)}}{\sqrt{x_1-b}(x_1-e)}\right)\cos\varphi(x_1)\right)\quad \text{for } x_1>b, \tag{A.1}$$

$$\sigma_{33}^{(1)}(x_1,0)+m_{14}D_3^{(1)}(x_1,0) = -\frac{1}{\sqrt{(x_1-c)(x_1-a)\gamma_1}2\pi}$$
$$\times\left[\left(\Psi_1\frac{\sqrt{(d-c)(b-d)}}{x_1-d}+\Psi_3\frac{\sqrt{(e-c)(b-e)}}{x_1-e}\right)(\exp[\varphi_0(x_1)]+\gamma_1\exp[-\varphi_0(x_1)])\right.$$
$$\left.+\left(\Psi_2\frac{\sqrt{(d-c)(b-d)}}{x_1-d}+\Psi_4\frac{\sqrt{(e-c)(b-e)}}{x_1-e}\right)\sqrt{\frac{x_1-a}{b-x_1}}(\exp[\varphi_0(x_1)]-\gamma_1\exp[-\varphi_0(x_1)])\right]$$
$$\text{for } x_1\in(a,b), \tag{A.2a}$$

$$\sigma_{33}^{(1)}(x_1,0)+m_{44}D_3^{(1)}(x_1,0) = -\sqrt{\frac{(d-c)(a-d)}{(x_1-c)(x_1-a)}}\frac{P_3}{\pi(x_1-d)}-\sqrt{\frac{(e-c)(a-e)}{(x_1-c)(x_1-a)}}\frac{m_{44}D}{\pi(x_1-e)}$$
$$\text{for } x_1\in(a,b), \tag{A.2b}$$

$$n_{13}\left[u_3'(x_1,0)\right]+n_{14}[\varphi'(x_1,0)]$$
$$=\frac{\cosh(\pi\varepsilon_1)}{\pi\gamma_1\sqrt{(x_1-c)(a-x_1)}}\left[\left(\Psi_1\cos\varphi_1(x_1)-\Psi_2\sin\varphi_1(x_1)\frac{Y(x_1)}{Y(d)}\right)\frac{\sqrt{(d-c)(a-d)}}{(x_1-d)}\right.$$
$$\left.+\left(\Psi_3\cos\varphi_1(x_1)-\Psi_4\sin\varphi_1(x_1)\frac{Y(x_1)}{Y(d)}\right)\frac{\sqrt{(e-c)(a-e)}}{x_1-e}\right]\quad \text{for } x_1\in(c,a), \tag{A.3a}$$

$$n_{43}\left[u_3'(x_1,0)\right]+n_{44}[\varphi'(x_1,0)]=\frac{1}{\pi}\left[\sqrt{\frac{(d-c)(a-d)}{(x_1-c)(a-x_1)}}\frac{P_3}{(x_1-d)}+\sqrt{\frac{(e-c)(a-e)}{(x_1-c)(a-x_1)}}\frac{m_{44}D}{(x_1-e)}\right]$$
$$\text{for } x_1\in(c,a), \tag{A.3b}$$

$$n_{11}\left[u_1'(x_1,0)\right]$$
$$=-\frac{1}{\pi\sqrt{\gamma_1(x_1-c)(x_1-a)}}\left[\left(\cosh\varphi_0(x_1)\Psi_1+\sinh\varphi_0(x_1)\Psi_2\sqrt{\frac{(x_1-a)(b-d)}{(b-x_1)(a-d)}}\right)\frac{\sqrt{(d-c)(a-d)}}{(x_1-d)}\right.$$
$$\left.+\left(\cosh\varphi_0(x_1)\Psi_3+\sinh\varphi_0(x_1)\Psi_4\sqrt{\frac{(x_1-a)(b-e)}{(b-x_1)(a-e)}}\right)\frac{\sqrt{(e-c)(a-e)}}{(x_1-e)}\right]\quad\text{for } x_1\in(a,b), \tag{A.4}$$

where

$$\varphi_0(x_1)=2\varepsilon_1\arctan\sqrt{\frac{(a-c)(b-x_1)}{(b-c)(x_1-a)}}.$$

References

Atkinson, C., 1977. Dynamic crack problems in dissimilar media. In: Sih, G.C. (Ed.), Mechanics of Fracture, vol. 4. Noordhoff International Publishing, Leyden, pp. 213–248.

Bleustein, J.L., 1968. A new surface wave in piezoelectric material. Appl. Phys. Lett. 13, 412–413.

Chen, Z.T., Karihaloo, B.L., Yu, S.W., 1998. A Griffith crack moving along the interface of two dissimilar piezoelectric materials. Int. J. Fract. 91, 197–203.

Comninou, M., 1977. The interface crack. J. Appl. Mech. 44, 631–636.

Eshelby, J.D., Read, W.T., Shockley, W., 1953. Anisotropic elasticity with application to dislocation theory. Acta Metall. 1, 251–259.

Gautesen, A.K., Dundurs, J., 1988. The interface crack under a combined loading. ASME J. Appl. Mech. 55, 580–586.

Gol'dstein, R.V., 1966. On the steady motion of a crack along a straight line boundary between two joined materials [in Russian]. Mech Tverdogo Tela 1, 94–102.

Gulyaev, Y.V., 1969. Electroacoustic surface waves in solids. Sov. Phis. JETP 9, 37–38.

Herrmann, K.P., Loboda, V.V., 1999. On interface crack models with contact zones situated in an anisotropic bimaterial. Arch. Appl. Mech. 69, 317–335.

Herrmann, K.P., Loboda, V.V., 2000. Fracture mechanical assessment of electrically permeable interface cracks in piezoelectric bimaterials by consideration of various contact zone models. Arch. Appl. Mech. 70, 127–143.

Herrmann, K.P., Loboda, V.V., 2003. Fracture mechanical assessment of interface cracks with contact zones in piezoelectric bimaterials under thermoelectromechanical loadings II. Electrically impermeable interface cracks. Int. J. Solids Struct. 40, 4219–4237.

Herrmann, K.P., Noe, A., 1992. Analysis of quasi-static and dynamic interface crack extension by the method of caustics. Eng. Fract. Mech. 42, 573–588.

Herrmann, K.P., Noe, A., 1993. Analysis of dynamic mixed-mode stress fields in bimaterials by the method of caustics. Theo. Appl. Fract. Mech. 19, 49–59.

Herrmann, K.P., Noe, A., 1995. Dynamic interface crack propagation and related problems of caustics. Arch. Mech. 47, 915–956.

Herrmann, K.P., Loboda, V.V., Govorukha, V.B., 2001. On contact zone models for an electrically impermeable interface crack in a piezoelectric bimaterial. Int. J. Fract. 111, 203–227.

Herrmann, K.P., Loboda, V.V., Komarov, A.V., 2004. Contact zone assessment for a fast growing interface crack in an anisotropic bimaterial. Arch. Appl. Mech. 74.

Huang, Y., Wang, W., Liu, C., Rosakis, A.J., 1998. Intersonic crack growth in bimaterial interfaces: an investigation of crack face contact. J. Mech. Phys. Solids 46, 2233–2259.

Lekhnitskii, S.G., 1963. Theory of Elasticity of an Anisotropic Elastic Body. Holden-Day, San Francisco.

Loboda, V.V., 1993. The quasi-invariant in the theory of interface cracks. Eng. Fracture Mech. 44, 573–580.

Muskhelishvili, N.I., 1977. Some Basic Problems of Mathematical Theory of Elasticity. Noordhoff International Publishing, Leyden.

Nakhmejn, E.L., Nuller, B.M., 1990. Dynamic contact problems for an orthotropic elastic half plane and a bimaterial plane. Priklad. Matemat. Mech. [in Russian] 54, 633–641.

Noe, A., Herrmann, K.P., 1993. Dynamische ausbreitung gekrümmter grenzflächenrisse. ZAMM 73, T469–T472.

Noe, A., Herrmann, K.P., 1997. Elastodynamic parameters for dynamic interface fracture mechanics. Acta Mech. 123, 203–226.

Parton, V.Z., Kudryavtsev, B.A., 1988. Electromagnetoelasticity. Gordon and Breach Science Publishers, New York.

Shen, S., Nishioka, T., Hu, S.L., 2000. Crack propagation along the interface of piezoelectric bimaterial. Theo. Appl. Fract. Mech. 34, 185–203.

Simonov, I.V., 1983. Dynamics of the tear-shear crack at the interface of two elastic materials. Rep. Acad. Sci. USSR [in Russian] 271, 65–68.

Simonov, I.V., 1985. The interface crack in homogeneous field of stresses [in Russian]. Mech. Comp. Mater., 969–976.

Stroh, A.N., 1958. Dislocations and cracks in anisotropic elasticity. Phil. Mag. 7, 625–646.

Suo, Z., Kuo, C.-M., Barnett, D.M., Willis, J.R., 1992. Fracture mechanics for piezoelectric ceramics. J. Mech. Phys. Solids. 40, 739–765.

Wang, X., Zhong, Z., Wu, F.L., 2003. A moving conducting crack at the interface of two dissimilar piezoelectric materials. Int. J. Solids Struct. 40, 2381–2399.

Williams, M.L., 1959. The stresses around a fault or cracks in dissimilar media. Bull. Seismol. Soc. Amer. 49, 199–204.

Willis, J.R., 1971. Fracture mechanics of interfacial cracks. J. Mech. Phys. Solids 19, 353–368.

Wu, K.C., 1991. Explicit crack tip fields of an extending interface crack in an anisotropic bimaterial. Int. J. Solids Struct. 27, 455–466.

Yang, W., Suo, Z., Shih, C.F., 1991. Mechanics of dynamic debonding. Proc. R. Soc. Lond. A. 433, 679–697.

Yoffe, E., 1951. The moving Griffith crack. Philos. Mag. 42, 739–750.